Investigation of location, electronic structures, and associated properties of chalcogen atoms adsorbed on silicon surfaces: Sulfur and selenium

S. M. Mohapatra, B. N. Dev,* K. C. Mishra,† W. M. Gibson, and T. P. Das
Department of Physics, State University of New York at Albany, Albany, New York 12222
(Received 13 January 1988)

The binding energies of four possible models for sulfur and selenium on the silicon (110) surface have been investigated by the Hartree-Fock cluster procedure. It is concluded that the most likely model for chalcogen atoms adsorbed on this surface is an interchain-bridge model with the adsorbed atom bonded to two atoms on adjacent chains on the surface. This model is shown to provide a Se—Si bond distance of 2.60 Å, in good agreement with the value of 2.55±0.05 Å from x-ray standing-wave measurements. Predictions are made for the ultraviolet photoemission spectra, vibrational frequencies and amplitudes, and nuclear quadrupole interactions associated with the adsorbed sulfur and selenium atoms. The results of the present investigation are shown to explain the intrachain-bridge position observed for tellurium on the silicon (111) surface.

I. INTRODUCTION

Adsorbate-covered semiconductor surfaces are currently a subject of extensive investigations by a number of different experimental techniques, among them, surface extended x-ray-absorption fine structure (SEXAFS),[1–4] x-ray standing wave (XSW),[5–9] ultraviolet photoemission spectroscopy (UPS),[10–13] x-ray photoemission spectroscopy (XPS),[14] scanning tunneling microscopy (STM),[15] kinematical total reflection Bragg diffraction (TRBD),[16] and radiative[17–20] hyperfine structure procedures. From these techniques valuable information has been obtained on the location[1,3,4,7–9] of the adatom, the local density of states,[10–13] vibrational[7,8] properties, and the interaction of the nuclear quadrupole moment of the adatom with its surroundings. So far the major experimental[3,4,10–13,21,22] efforts on adsorbed atoms have involved hydrogen and halogen atoms. However, experimental results[3,9] on the locations of a number of chalcogen atoms on semiconductor surfaces have recently become available through the use of SEXAFS and XSW techniques. Among these adsorbed systems are tellurium on silicon and germanium[3] and selenium on silicon.[9] Currently, theoretical investigations to understand these systems have been carried out by a number of techniques. Thus, the cluster technique[23–33] using the Hartree-Fock self-consistent procedure has been applied to adsorbed hydrogen,[24] oxygen,[25] and halogen[23,26–29,34] systems, fluorine through iodine, using all-electron calculations for the lighter atoms[27,28] and pseudopotential techniques for the heavier[26,27,34] halogens. The Green's function[10] technique has been applied to chlorine atoms on silicon surfaces. Both the cluster technique and the Green's function technique have been successful in explaining locations of halogen atoms above the silicon surface as well as UPS data wherever available. Theory has also been applied to study vibrational effects[26] such as amplitudes and frequencies for vibrations of adsorbed atoms, and comparison has been made with the limited experimental results available. The electronic structures obtained by the Hartree-Fock cluster technique have been utilized to predict the nuclear quadrupole interaction energies[26,28,34,35] for the nuclei of all the halogen atoms. No experimental data are currently available to test these predictions. However, beam-foil[20] and perturbed angular correlation[18,19] techniques are currently being used for studying these properties for metallic surfaces, and it appears that these techniques may soon become applicable to semiconductor surfaces as well.

The chalcogen-adsorbed systems differ from the halogen systems in the important respect that the adsorbed atoms occupy more complicated positions than the atop positions found for the halogen atoms on semiconductor surfaces. The experimental measurements[3] carried out by the SEXAFS technique for tellurium on silicon, and germanium (111) surfaces suggest that the adsorbed atom is bonded to two surface host atoms. A similar conclusion has been reached from the measurements of selenium on silicon (111) and (110) surfaces by the XSW technique.[9]

The present work deals with Hartree-Fock cluster investigations on sulfur and selenium atoms absorbed on the (110) surface of silicon. The selenium investigations were prompted by observations regarding the Se—Si bond distances from (XSW) measurements[9] on (110) and (111) surfaces. Our investigations for the (110) surface using a number of different geometries for the selenium atom allow one to draw conclusions about its expected locations on both (110) and (111) surfaces and to make comparisons with the experimentally observed bond distances.[9] Additionally, as in the case of our investigations on adsorbed halogen atoms[26–28,34] we have also made predictions regarding the expected ultraviolet photoemission spectra (UPS), the ^{79}Se nuclear quadrupole interaction tensor, and vibrational properties associated with the selenium atom. While no experimental results are currently available for these properties, they are expected

to become available in the near future, and comparison with theory will be able to provide a detailed test of the calculated electronic structure. The investigations on sulfur were carried out both to study systematic variations in properties between these two isoelectronic (valence shell) systems and also to make comparisons with experimental data when they become available.

In Sec. II a brief description will be presented of the theoretical procedures used in this work for investigations of electronic structures and the associated properties that we have analyzed. The geometries of the clusters that we have utilized will also be discussed. Section III will deal with our results for the expected binding sites for the two atoms and comparison with results from XSW measurements for selenium. Results will also be presented for the UPS spectra, vibrational properties associated with the adsorbed atoms, and the ^{33}S and ^{79}Se nuclear quadrupole interaction tensors. Finally, Sec. IV will present the conclusions from the results of our work and their implications for the heavier chalcogen atom—tellurium.

II. PROCEDURE

As in our earlier work[26–28] on adsorbed halogen atoms at semiconductor surfaces, the energy levels and eigenfunctions are obtained by the Hartree-Fock procedure using a cluster to represent the adsorbed atoms, the surface atoms of the host and their neighbors. As before, to enhance the speed of computation, STO-3G basis[36] sets with each Slater orbital expanded in terms of three normalized Gaussian functions were used for the variational approach to the Hartree-Fock procedure. The use of a more extensive basis set would have been preferable but this was difficult to do with our available computing facilities especially because we wanted to include sizable numbers of atoms in the clusters chosen. However, earlier work[26,27,32] using this choice of basis set for halogen atoms adsorbed on Si and for molecules containing halogen atoms have provided good agreement with the observed bond distances between the adsorbed atoms and surface atoms and with results of a calculation[23] using a more extensive basis set. Good agreement has also been found[27] between positions of peaks in the calculated densities of states and experimental ultraviolet photoemission data.

A major aspect of the present investigations is the determination as to which of a number of possible geometries is energetically most favorable for the adsorbed atom. One has therefore to (a) study the minimum energy configurations[26,27,34] for each geometry and (b) make a decision[23] regarding the most stable one among these geometries. For (a), for instance, when one is interested in the host-adatom bond distance for the adsorbate atom in the atop position for halogens, one can use total energy curves,[26,27,34] while for (b), since the clusters for different geometries involve different numbers of atoms, one has to compare binding energies for the adsorbate atoms rather than the total energies of the clusters. The binding energy D_e for an adsorbate atom can be defined by the relation[23,32]

$$D_e=\frac{1}{n}[(E_b+E_n)-E_c]\ , \tag{1}$$

where E_c refers to the energy of a cluster with n adsorbate atoms, E_b that for the same cluster without the adsorbate atoms, and E_n the total energy of n free adsorbate atoms. The calculated Hartree-Fock energies have been used for these quantities in Eq. (1). If one had used for the free-atom energies E_n, values obtained from experimental ionization energies,[37] then one would be including correlation corrections to the E_n. This would be inappropriate to do, since correlation effects are rather difficult to include in the other terms in Eq. (1).

The different geometrical configurations that we have examined for the adsorbed S and Se atoms can be best understood by referring to Fig. 1 which represents two adjacent chains of Si atoms on a (110) surface. For a (110) plane inside the bulk, each atom in the chain is tetrahedrally bonded to four other atoms, two on the plane (for instance, A_1 and C_1 for the atom B_1) and two other atoms, one above the plane in question and one below. For the surface, the plane above is absent, so that there is a dangling bond associated with every atom as shown by the broken lines in Fig. 1. Two of the possible configurations that we have considered for the adsorbed S or Se atom can be described as atop positions. For one of them, the chalcogen atoms are attached to the dangling bonds on two adjacent surface atoms belonging to a particular chain, such as, for instance, atoms A_1 and B_1. Another possible atop configuration, referred to as atop two, would correspond to having two chalcogen atoms attached to dangling bonds belonging to adjacent atoms on two neighboring chains. Two chalcogen atoms in atop positions are considered at a time because of the divalent nature of these atoms with two holes in the valence shell and the desirability to have the clusters simulating the adsorbed atoms and the surface as being diamagnetic with an even number of electrons. A third configuration, that appears to be a probable one, can be described as involving a single chalcogen atom attempting to saturate two dangling bonds on next-nearest-neighbor atoms on a single chain such as A_1 and C_1 in Fig. 1. The reason that

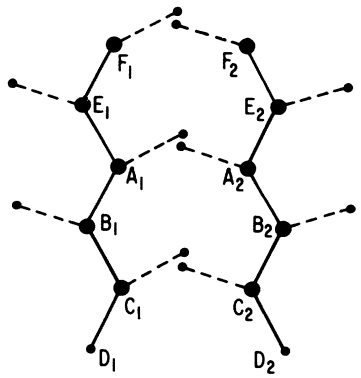

FIG. 1. Atomic arrangements and the dangling bonds on surface chains on the silicon (110) surface.

this configuration seems more probable than one involving the chalcogen atom bonded to two nearest-neighbor atoms on a chain, for instance A_1 and B_1, is that in the latter case, the two dangling bonds are rather twisted with respect to each other in contrast to the parallelism of such bonds on next-nearest-neighbor atoms. This model will be referred to in the rest of the paper as the intrachain model. The fourth and last model we have analyzed, and which appears from our results to be the most likely one for the (110) surface, will be referred to as the interchain model involving the adsorbed chalcogen atom bonded to two adjacent Si atoms on neighboring chains, for instance A_1 and A_2 or C_1 and C_2 in Fig. 1.

The clusters that we have used for our Hartree-Fock investigations for these four models are given in Figs. 2(a)–2(d). As in earlier cluster calculations, including ours[26–28,34] on adsorbed halogen systems, saturator hydrogens[29–35,38] are used to simulate the rest of the solid outside of the cluster. Of the four clusters in Figs. 2(a)–2(d), the first two represent the two atop models with adsorbed atoms bonded to two adjacent host atoms on the same chain and neighboring chains, respectively. Figure 2(c) represents the intrachain-bridge model with the chalcogen atom bonded to two silicon atoms on the same chain which are second-nearest neighbors to each other. Figure 2(d) represents the interchain-bridge model with the chalcogen atoms bonded to silicon atoms on neighboring chains. Since we have used the binding energies of the adsorbed atoms as given by Eq. (1) as the criteria to determine the most likely binding site, we need accurate evaluations of the differences between the total energies of the two clusters with and without the adsorbed atom present. We have therefore carried out all-electron Hartree-Fock calculations rather than calculations using pseudopotentials as was done earlier[26] for the heavier halogen-adsorbed systems. In view of this, the largest clusters that we could handle with the appropriate symmetries for the four models are the ones shown in Figs. 2(a)–2(d). Thus, for instance, for the atop model in Fig. 2(a), if we had replaced two of the hydrogen atoms attached to atom B_1 and A_1 by the surface host atoms C_1 and D_1 (in the nomenclature of Fig. 1) and saturated the dangling bonds for these latter two atoms by Se, the enlarged cluster including the saturator hydrogens would involve four Si atoms, four Se, and six hydrogen atoms with a total of 198 electrons and 114 basis functions which would have required excessive computational time with the computing facilities available to us. In the three other figures in Fig. 2 we have also used the nomenclature of Fig. 1 for the host atoms on the surface. The unlabeled host atoms in Figs. 2(b) and 2(d) refer to atoms below the surface. From our investigations on adsorbed halogen systems[26,28,35] where we have compared one-electron properties obtained from all-electron cluster calculations with similar numbers of atoms as in Figs. 2(a)–2(d) and from larger clusters using pseudopotential methods, there is support for the expectation that the conclusions obtained from the clusters in Fig. 2 in the present work would be reliable.

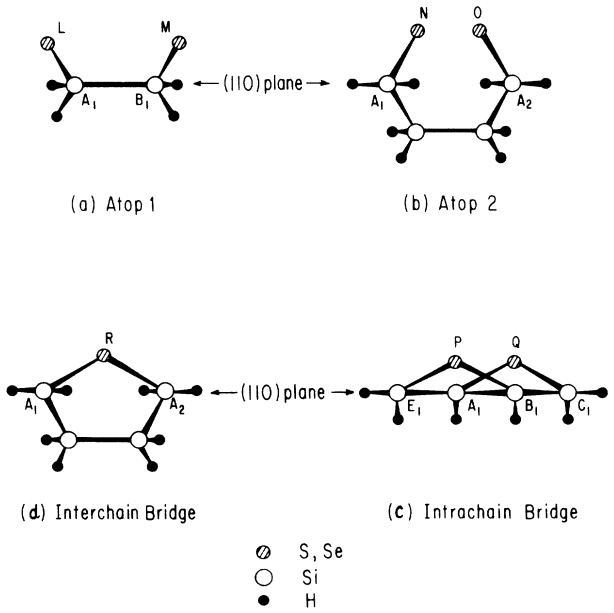

FIG. 2. Clusters used for the different models chosen for the chalcogen adsorption on the silicon (110) surface. The host atoms are named according to the nomenclature in Fig. 1. Cluster (a) refers to the model atop 1, (b) to atop 2, (c) to the intrachain model, and (d) to the interchain model.

We turn next to the procedures for evaluation of properties associated with the adsorbed chalcogen atoms. For the determination of the equilibrium positions of the S and Se, for all four clusters, we have carried out a minimization of the total energies which occur in the binding energy expression in Eq. (1) with respect to displacements of the adsorbed atoms made in keeping with the symmetries of the clusters involved. Thus for the atop-one and atop-two positions in Figs. 2(a) and 2(b) simultaneous changes have been carried out for the Si—S(Se) bond distances represented by (A_1L, B_1M) and (A_1N, A_2O), respectively, these lines being along the tetrahedrally directed bond directions at A_1, A_2, and B_1. For the intrachain-bridge model in Fig. 2(c), we have considered displacements of the adsorbed atoms P and Q perpendicular to the lines joining the surface host atoms E_1 and B_1, and A_1 and C_1, respectively. Correspondingly for the interchain-bridge model, variations in the perpendicular distance between R and the line joining A_1 and A_2 were considered. As will be discussed in Sec. III dealing with our results, binding energy considerations favored the interchain-bridge model as the most likely one among the four models we have studied.

For the rest of the properties studied in this work, the same general methods[26–28,32] have been adopted as in our earlier work on adsorbed halogen atom systems. Thus, for obtaining the density-of-states curve to examine the positions of the peaks which can be compared with the results from UPS measurements, a Lorentzian broadening[39] procedure has been applied to obtain a continuous distribution in energies. The following expression has been used for the computation of the density of states:

$$D(E)=\sum_n \frac{\lambda/\pi}{(E-E_n)^2+\lambda^2}\ , \tag{2}$$

where the E_n's are the discrete energy levels determined from the Hartree-Fock calculations and λ is a broadening parameter. For the vibrational frequencies, the force constants k in the frequency expression,

$$\omega=(k/m)^{1/2} \tag{3}$$

were determined for the four models from the second derivatives of the energy curves obtained in the minimization procedure discussed earlier, m referring to the mass of the adsorbed atom. There would be some correction to m if one considered the motions of the surface Si atoms. This is a rather complicated question and will have to be addressed critically in the future in obtaining accurate results for comparison with experiment when vibrational frequencies become available. At the present time, we are interested only in making approximate predictions for these frequencies. For the vibrational amplitudes associated with the motions of the adsorbed atoms, we have obtained the mean-square displacements $\langle u^2\rangle$ for the four models using the expression[26,32]

$$\langle u^2\rangle=\left[\frac{\hbar}{m\omega}\right]\left\{\tfrac{1}{2}+1\Big/\left[\exp\left[\frac{\hbar\omega}{k_BT}\right]-1\right]\right\} \tag{4}$$

involving Boltzmann averaging over the various vibrational states at any temperature T. In making comparisons with experimental data on the vibrational amplitudes, when they become available, one would have to allow for vibrational motions of the surface host atoms. Assuming these vibrational motions to take place along the dangling bond directions, one can use the expression[26,32]

$$\langle u_{\rm eff}^2\rangle=\langle u^2\rangle+\langle u_s^2\rangle \tag{5}$$

for the two atop positions considered in Figs. 2(a) and 2(b) while for the bridge positions, the corresponding expression would be

$$\langle u_{\rm eff}^2\rangle=\langle u^2\rangle+4\langle u_s^2\rangle\langle\cos^2\theta\rangle\ , \tag{6}$$

where θ refers to the angles between the lines PE_1 and PA_1 or (QA_1 and QB_1) in Fig. 2(c) and between the lines RA_1 and the perpendicular drawn from R on the line joining A_1 and A_2 in Fig. 2(d). It appears to be a reasonable approximation to replace $\langle\cos^2\theta\rangle$ by $\cos^2\theta_0$, θ_0 being the equilibrium value of θ.

The last electronic property that we have studied is the nuclear quadrupole interaction[40] associated with the adsorbed atoms at the surface. Unlike the case of halogen atoms at the atop position on Si that we have studied earlier where there is axial symmetry in the electron distribution around the halogen atom, in the case of chalcogen atoms on the (110) surface, Figs. 2(a)–2(d) indicate that there should be a strong departure from axial symmetry. One therefore expects a finite asymmetry parameter η in the electric-field gradient at the adsorbate nucleus, given by[40]

$$\eta=\frac{V_{x'x'}-V_{y'y'}}{V_{z'z'}}\ , \tag{7}$$

where $V_{i'i'}$ refer to the principal components of the field-gradient tensor. The maximum principal component $V_{z'z'}$ is denoted in the literature by q, the quantity e^2qQ, where eQ is the nuclear quadrupole moment, being referred to as the nuclear quadrupole coupling constant. The X' and Y' axes are chosen according to the usual convention that $|V_{x'x'}|<|V_{y'y'}|<|V_{z'z'}|$ which assures that η lies within 0 and 1. To determine the principal components and the principal axes, we have used the standard procedure[40] of obtaining the nine field-gradient tensor components V_{ij} given by

$$V_{ij}=\sum_n \xi_n\frac{(3x_{Ni}x_{Nj}-r_N^2\delta_{ij})}{r_N^5}-\sum_\mu\frac{\langle\psi_\mu|\,3x_ix_j-r^2\delta_{ij}\,|\psi_\mu\rangle}{r^5} \tag{8}$$

in any chosen coordinate system (i,j running over x, y, and z) and then diagonalizing the calculated $\overleftrightarrow{V}$ tensor. In Eq. (8), N refers to the nuclei (nuclear charge ξ_n) of all other atoms in the cluster except the adsorbed atom and x_{Ni} refers to the coordinates of these nuclei with respect to the adsorbed-atom nucleus. In the second term, the x_i refer to the corresponding coordinates for the electrons in the system, and ψ_μ the electronic wave functions for all the occupied molecular orbital states of the cluster. Since these ψ_μ for both the corelike and valence orbitals are obtained by the Hartree-Fock procedure, the core orbitals are already distorted by electrostatic interaction with the nonspherical charge distributions associated with the valence electrons. The Sternheimer antishielding effects[41] associated with the core electrons are thus directly included when one evaluates the V_{ij} using Eq. (8), obviating the need to introduce any parameters[42] to incorporate these effects. Since it is the quadrupole coupling constant e^2qQ that is measured experimentally and not q, one needs a knowledge of the quadrupole moment Q of the host nucleus of interest. For $Q(^{33}\mathrm{S})$ and $Q(^{79}\mathrm{Se})$ we have used the tabulated values[43] of 0.05 and 0.8 b, respectively, which represent the averages of measured values by a number of different experimental techniques.

III. RESULTS AND DISCUSSION

The binding energies for the different sites shown in Figs. 2(a)–2(d) are listed in Table I. These binding energies have been obtained through the use of Eq. (1) for the total energies corresponding to the minima of the energy curves for the various clusters plotted as a function of the positions of S and Se atoms. Thus, for the atop position in Fig. 2(a), the configuration coordinate, with respect to which energy variation is studied, corresponds to the distances A_1L and B_1M between the surface Si atoms and adsorbed chalcogen atoms, both of which are simultaneously varied by equal amounts. For the atop-two configuration in Fig. 2(b), the configuration coordinate similarly corresponds to the distances A_1N and A_2O which are also varied simultaneously by equal amounts. For the intrachain-bridge site in Fig. 2(c) the configuration coordinates correspond to the bond distances of the adsorbed atoms P and Q from the Si atoms B_1 and E_1

TABLE I. Optimized Si—S(Se) bond distances and the binding energies for different models for S and Se atoms adsorbed on Si(110) surface.

Model	Bond distances (Å)		Binding energies D_e (eV/atom)	
	Si—S	Si—Se	S	Se
Atop 1	2.02	2.15	1.35	3.11
Atop 2	2.23	2.26	1.85	3.47
Intrachain	2.48	2.58	1.82	4.43
Interchain	2.56	2.60	3.77	6.71

and A_1 and C_1, respectively, on the (110) surface. From symmetry considerations the bond distances PB_1 and PE_1 are taken to be equal to each other and to QA_1 and QC_1, so that there is just one configuration coordinate. Lastly, for the interchain-bridge situation corresponding to Fig. 2(d), the configuration coordinate is the height of the adsorbed chalcogen atom R over the surface.

From Table I the interchain-bridge site is seen to be clearly the one with the highest binding energy for both S and Se. For S, the next two models in terms of stability are the atop-2 and the intrachain model while atop 1 has the lowest binding energy. In looking for the physical factors which influence the relative strengths of binding of the adsorbed atoms at these different sites, we notice that adatom-adatom interaction does not appear to be particularly important for the binding of the adsorbed atoms to the surface. Thus, comparing the atop-1 and atop-2 sites, the separations of the two adatoms in Figs. 2(a) and 2(b) are, respectively, 4.2 and 2.5 Å. The former is too large for significant adatom-adatom interaction. The latter is somewhat larger than the equilibrium distance of 1.9 Å for a free S_2 molecule. So there could be a small but significant bonding between the adatoms N and O in Fig. 2(b). The fact that the binding energies for the atop-one and atop-two positions in Table I are not very different indicates that the influence of the bonding between N and O is less significant than that between the surface atoms and the adatoms in determining the binding of the latter to the surface. In the intrachain bridge model in Fig. 2(c), the adatom-adatom interaction is also not expected to be too significant because the adatom-adatom separations are also rather large, namely 3.7 Å. The stronger binding of the adatom to the surface in the interchain model as compared to the intrachain model, even though in both cases the adatom is bonded to two surface atoms, can be understood by an examination of Fig. 1. Thus, the bonds A_1R and A_2R in Fig. 2(d) for the interchain model arise out of dangling bonds that are directed much more closely towards each other than is the case for the bonds E_1P and B_1P in Fig. 2(c), there being thus substantially greater twisting of the corresponding dangling bonds in Fig. 1 in the latter case. As a by-product of this observation, one can justify our not considering the twisting of the bonds A_1L and B_1M in Fig. 2(a) and A_1N and A_2O in Fig. 2(b) for the atop-1 and atop-2 models from the corresponding tetrahedrally directed dangling bonds in Fig. 1, since this would be expected to lead to smaller binding energies for the adatoms than those in Table I. These physical considerations for the binding of the adsorbed surface atoms also apply for Se. The trends in binding energies for the Se system are indeed seen to be similar to that for S except for one difference. The order of the binding energy for atop-2 and intrachain models appears to be reversed as compared to S. This interesting change in the order of stability is probably the result of differences in bonding between the adsorbed and the host surface atoms due to variations in the relative sizes of their orbitals.

The calculated host-adsorbed atom-bond [Si—S(Se)] distances are also listed in Table I. The only system for which the bond distance has been measured is Se on Si, where the XSW technique[9] provides a Se—Si bond distance of (2.55±0.05) Å. It is gratifying that the calculated bond distance of 2.60 Å for the interchain-bridge model, which has been found to have the highest binding energy, agrees very well with the observed experimental[9] bond distance and lends support to the conclusion regarding this model being the appropriate one for the chalcogens adsorbed on Si(110) surface. There is no experimental bond-distance measurement available for S on the Si(110) surface. If one subtracts the difference of 0.14 Å between the atomic radii of S and Se from the Se—Si distance, this would suggest that the S—Si distance have an upper limit of 2.54 Å. This latter result is quite close to the calculated S—Si bond distance shown in Table I for the interchain model. It will be helpful to have actual measurements of the S—Si distance by any of the available experimental techniques[1–9] for a better comparison with the prediction from theory in the present work.

From the results of our calculations on chalcogen atoms on the Si(110) surface, it is also possible to draw conclusions about the likely configuration of chalcogen atoms adsorbed on the Si(111) surface. Of the four models considered for chalcogen atoms on the Si(110) surface, only two, namely the intrachain-bridge model and the atop-one model can occur for the (111) surface. From the binding energies in Table I, it is clear that of these two, the more stable model and therefore the most likely one for the (111) surface is the position bridging two surface nearest-neighbor Si atoms corresponding to the (intrachain-bridge) model. This conclusion agrees with that for Se on the Si(111) surface from XSW measurements[9] and for tellurium on the Si(111) surface from SEXAFS (Ref. 3) measurements.

Turning next to the local density-of-states curves obtained for the four different clusters representing adsorption of chalcogen atoms at different sites on the Si(110) surface as shown in Figs. 3(a) and 3(b), we obtain in all

four cases, sets of peaks whose compositions are as follows. The peaks around -15 eV or below have primarily S(3s)- or Se(3s)-like character, those around -12 eV involve σ bonding of S or Se with Si, and the peaks around -10 eV have Si(3s) character. The strong peak near -5 eV involves predominantly the 1s orbitals of H at the cluster boundaries which have been used for embedding purposes. These strong peaks thus represent an artifact of the cluster calculation. The peaks in the region between 0 and -5 eV involve primarily π bonding between S or Se with Si and those above the Fermi energy are associated with S or Se π-like orbitals. The constituents of the various peaks in the LDOS curve are very similar for both S and Se, but the peak positions for Se are slightly shifted from those of S. Unfortunately, no UPS results are currently available for making a comparison to our computed LDOS. Such a comparison would provide a valuable check on the electronic structure calculations in the present work and provide another way of verifying the choice of the interchain model for the (110) surface determined here from binding energy considerations.

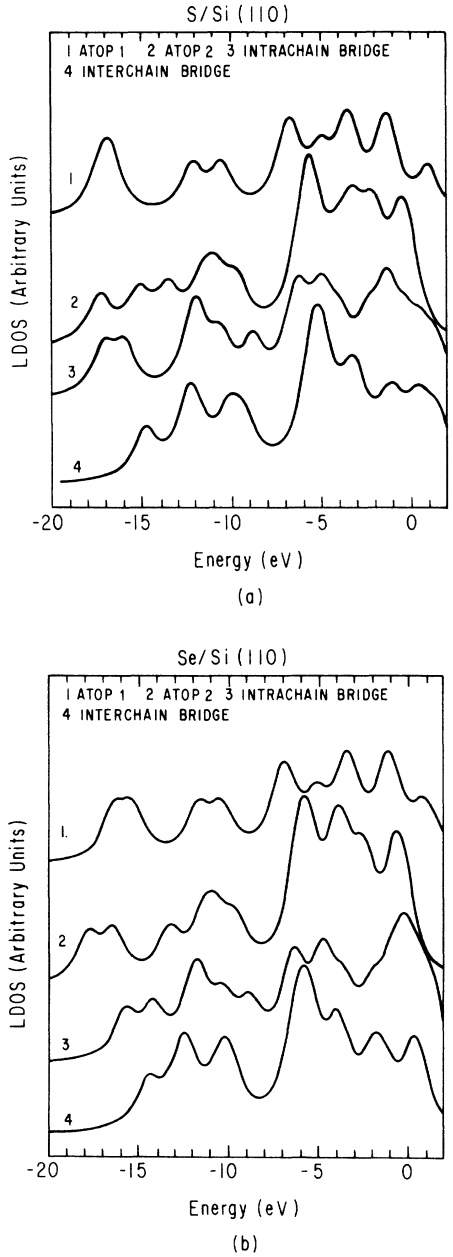

FIG. 3. Local density-of-states (LDOS) curves for different models chosen for (a) sulfur and (b) selenium adsorbed on the silicon (110) surface.

TABLE II. Vibrational frequencies (ω) and thermal vibrational amplitudes $(\langle u^2\rangle_{\text{eff}})^{1/2}$ for the clusters chosen for the various models.

	ω (cm^{-1})		$(\langle u^2\rangle_{\text{eff}})^{1/2}$ (Å)	
Model	S	Se	S	Se
Atop 1	503	264	0.1163	0.1150
Atop 2	394	234	0.1166	0.1151
Intrachain	327	223	0.1438	0.1506
Interchain	333	196	0.1101	0.1153

The other properties that we have calculated are the vibrational frequencies and the amplitudes associated with the vibrational motion for all the models that we have investigated for chalcogen adsorption on Si(110) surfaces. Equation (3) was used for the vibrational frequencies, with the force constant k determined from the total energy curves associated with the positions of the adsorbed atom. The vibrational amplitudes for the two atop positions have been calculated from Eq. (5) and those for the bridge positions from Eq. (6). The calculated values for these amplitudes are presented together with frequencies in Table II. Unfortunately, again there are no experimental data available to compare with the prediction in Table II, especially for the interchain model, which from our preceding discussions is expected to be the most likely one. However, information on the vibrational amplitude is available for a related system bromine[7,8] on germanium surface from XSW measurements using synchrotron radiation. The value of $(\langle u^2\rangle_{\text{eff}})^{1/2}$ in this latter system was found to be (0.067±0.053) Å which is close to our predicted value for the interchain-bridge model for Se on the Si surface in Table II.

The last property that we have investigated using the calculated HF wave functions refers to the nuclear quadrupole interaction tensors for both ^{33}S and ^{79}Se using the procedure described in Sec. II. Table III presents the re-

TABLE III. Nuclear quadrupole interaction parameters for S and Se adsorbed on the Si(110) surface.

	e^2qQ (MHz)		η	
Model	S	Se	S	Se
Atop 1	42.98	806.31	0.44	0.43
Atop 2	45.77	856.47	0.54	0.58
Intrachain	42.15	759.35	0.56	0.66
Interchain	43.16	758.64	0.76	0.92

sults for the quadrupole coupling constant e^2qQ and the asymmetry parameters η [Eq. (7)] for both ^{33}S and ^{79}Se nuclei for all the four models that we have examined for chalcogen adsorption on the Si(110) surface. In contrast to the case of halogens on the Si(111) surface where there was axial symmetry about the adsorbate atom nucleus, in the present case none of the four possible models have axial symmetry and therefore lead to finite values for η. The values of e^2qQ and η, especially the latter, are found to depend sensitively on the models chosen. For both S and Se, the value of η is found to be largest for the interchain models. It is hoped that experimental results for e^2qQ and η will become available in the near future from either double-resonance[44]-type measurements or by the beam-foil[20] technique, which has been recently applied to adsorbed nuclei at metallic surfaces. A comparison between theory and experiment of e^2qQ and η would allow another test about the selection of the interchain-bridge model as the most likely one for chalcogens on Si(110) surface from the results of our binding energy calculations.

IV. CONCLUSION

Using four different models for the location of the chalcogen atoms, sulfur and selenium on the (110) surface of silicon, and investigating the binding energy of the chalcogen atoms for each of these models, it has been demonstrated that the most likely location of the adsorbed chalcogen atoms is in an interchain-bridge position, with the chalcogen atom bonded to two atoms on adjacent chains. For this position, the bond distance between the Se atom and the nearest two Si atoms was found to be 2.60 Å in good agreement with the experimental result (2.55±0.05) Å found from XSW measurements.[9] For the (111) surface, for which the interchain-bridge position cannot occur, an intrachain position with the chalcogen atom equally bonded to two neighboring atoms on the same chain is found to be the most likely one, a conclusion in agreement with observations from SEXAFS[3] measurements for tellurium and XSW[9] measurements for selenium on the Si surface. Predictions are made for the expected UPS spectra, vibrational frequencies and amplitudes, and nuclear quadrupole interactions associated with S and Se on the (110) surface of Si. It is hoped that experimental data for these properties will be available in the near future to test these predictions and provide a more comprehensive test of our conclusions regarding the models for chalcogen atoms adsorbed on silicon surfaces. On the theoretical side, while it is not likely to change the conclusion from binding energy considerations about the likely locations of the chalcogen atoms on the Si(110) and (111) surfaces, it would be helpful, from the point of view of quantitative comparison of theory and experiment concerning properties of chalcogen atoms adsorbed on these surfaces, to attempt improvements in the future involving larger clusters and inclusion of lattice-relaxation effects. Such investigations would be rather time consuming on conventional computers but should be practicable with supercomputing facilities.

---

*Present address: Hamburger Synchrotronstrahlungslabor HASYLAB at DESY, D-2000, Hamburg 52, Federal Republic of Germany.

†Present address: Lighting Products Group, GTE Sylvania, 100 Endicot Street, Danvers, MA 01923.

[1]P. H. Citrin, P. Eisenberger, and R. C. Hewitt, Phys. Rev. Lett. **41**, 309 (1978).

[2]P. A. Lee, P. H. Citrin, P. Eisenberger, and B. M. Kincaid, Rev. Mod. Phys. **53**, 769 (1981).

[3]P. H. Citrin, P. Eisenberger, and J. E. Rowe, Phys. Rev. Lett. **48**, 802 (1982).

[4]P. H. Citrin, J. E. Rowe, and P. Eisenberger, Phys. Rev. B **28**, 2299 (1983).

[5]J. A. Golovchenko, J. R. Patel, D. R. Kaplan, P. L. Cowan, and M. J. Bedzyk, Phys. Rev. Lett. **49**, 560 (1982).

[6]M. J. Bedzyk, W. M. Gibson, and J. A. Golovchenko, J. Vac. Sci. Technol. **20**, 634 (1982).

[7]G. Materlik and J. Zegenhagen, Phys. Lett. **104A**, 47 (1984).

[8]M. J. Bedzyk and G. Materlik, Phys. Rev. B **31**, 4110 (1985).

[9]B. N. Dev, T. Thundat, and W. M. Gibson, J. Vac. Sci. Technol. A **3**, 946 (1985).

[10]M. Schlüter, J. E. Rowe, G. Margaritondo, K. M. Ho, and M. L. Cohen, Phys. Rev. Lett. **37**, 1632 (1976).

[11]J. E. Rowe, G. Margaritondo, and S. B. Christman, Phys. Rev. B **16**, 1581 (1977).

[12]G. Margaritondo, J. E. Rowe, and S. B. Christman, Phys. Rev. B **14**, 5396 (1976).

[13]K. C. Pandey, T. Sakurai, and H. D. Hagstrum, Phys. Rev. B **16**, 3648 (1977).

[14]T. A. Carlson, *Photoelectron and Auger Spectroscopy* (Plenum, New York, 1975).

[15]G. Binnig, H. Rohrer, C. Gerber, and E. Weibel, Phys. Rev. Lett. **50**, 120 (1983).

[16]P. Eisenberger and W. C. Marra, Phys. Rev. Lett. **46**, 1081 (1981).

[17]T. Yang, A. Krishnan, N. Benczer-Koller, and G. Bayruther, Phys. Rev. Lett. **48**, 1292 (1982).

[18]W. Korner, W. Keppner, B. Lechndorff-Junges, and G. Schatz, Phys. Rev. Lett. **49**, 1735 (1982).

[19]T. Klas, J. Voigt, W. Keppner, R. Wesche, and G. Schatz, Phys. Rev. Lett. **57**, 1068 (1986).

[20]B. Horn, E. Koch, and D. Fick, Phys. Rev. Lett. **53**, 364 (1984).

[21]Y. J. Chabal, Phys. Rev. Lett. **50**, 1850 (1983).

[22]K. Fujiwara, Phys. Rev. B **24**, 2240 (1981).

[23]M. Seel and P. S. Bagus, Phys. Rev. B **28**, 2023 (1983).

[24]K. Hermann and P. S. Bagus, Phys. Rev. B **20**, 1603 (1979); M. Seel and P. S. Bagus, *ibid.* **23**, 5464 (1981).

[25]I. P. Batra, P. S. Bagus, and K. Hermann, Phys. Rev. Lett. **52**, 384 (1984).

[26]S. M. Mohapatra, N. Sahoo, B. N. Dev, K. C. Mishra, W. M. Gibson, and T. P. Das, J. Vac. Sci. Technol. A **4**, 2441 (1986).

[27]B. N. Dev, K. C. Mishra, W. M. Gibson, and T. P. Das, Phys. Rev. B **29**, 1101 (1984).

[28]K. C. Mishra, B. N. Dev, S. M. Mohapatra, W. M. Gibson, and T. P. Das, Hyperfine Interact. **15/16**, 997 (1983).

[29]F. Illas and J. Rubio, Phys. Rev. B **31**, 8068 (1985).
[30]A. Redondo and W. A. Goddard III, and T. C. McGill, J. Vac. Sci. Technol. **21**, 649 (1982), and references to earlier work therein.
[31]P. Cremaschi and J. L. Whitten, Phys. Rev. Lett. **46**, 1242 (1981).
[32]B. N. Dev, S. M. Mohapatra, K. C. Mishra, W. M. Gibson, and T. P. Das, Phys. Rev. D **36**, 2666 (1987).
[33]N. Sahoo, S. K. Mishra, K. C. Mishra, A. Coker, T. P. Das, C. K. Mitra, L. C. Snyder, and A. Glodeanu, Phys. Rev. Lett. **50**, 913 (1983); N. Sahoo, S. K. Mishra, K. C. Mishra, T. P. Das, A. Coker, C. K. Mitra, L. C. Snyder, and A. Glodeanu, Hyperfine Interact. **17/19**, 525 (1984); N. Sahoo, K. C. Mishra, and T. P. Das, Phys. Rev. Lett. **55**, 1506 (1985).
[34]S. M. Mohapatra, B. N. Dev, N. Sahoo, K. C. Mishra, W. M. Gibson, and T. P. Das, Phys. Rev. B (to be published).
[35]S. M. Mohapatra, B. N. Dev, K. C. Mishra, W. M. Gibson, and T. P. Das, Hyperfine Interact. **34**, 581 (1987).
[36]W. J. Pietro, B. A. Levi, W. J. Hehre, and R. F. Stewart, Inorg. Chem. **19**, 2225 (1980); W. J. Hehre, R. Ditchfield, R. F. Stewart, and J. A. Pople, J. Chem. Phys. **52**, 2769 (1970); W. J. Hehre, R. F. Stewart, and J. A. Pople, *ibid.* **51**, 2657 (1969).
[37]H. Basch, A. Viste, and H. B. Gray, Theor. Chim. Acta (Berlin) **3**, 458 (1965); C. J. Ballhausen and H. B. Gray, *Molecular Orbital Theory* (Benjamin, New York, 1968).
[38]B. Cartling, B. Roos, and U. I. Wahlgren, Chem. Phys. Lett. **58**, 1066 (1973).
[39]B. Lindgren and D. E. Ellis, Phys. Rev. B **26**, 636 (1982).
[40]T. P. Das and E. L. Hahn, *Nuclear Quadrupole Resonance Spectroscopy* (Academic, New York, 1957).
[41]R. Sternheimer, Phys. Rev. **80**, 102 (1950); **84**, 244 (1951).
[42]T. P. Das and P. C. Schmidt, Z. Naturforsch. **41a**, 47 (1986).
[43]The values $Q(^{33}\mathrm{S})=0.05$ b and $Q(^{79}\mathrm{Se})=0.8$ b are taken from G. H. Fuller and V. W. Cohen, *Nuclear and Atomic Data Tables* (Academic, New York, 1969), Vol. 5.
[44]A. G. Redfield, Phys. Rev. **130**, 589 (1963).